Available online at www.sciencedirect.com
SCIENCE DIRECT
Journal of Power Sources 156 (2006) 321–333
JOURNAL OF POWER SOURCES
www.elsevier.com/locate/jpowsour

Techno-economic modelling of a solid oxide fuel cell stack for micro combined heat and power

A.D. Hawkes [a,*], P. Aguiar [b], C.A. Hernandez-Aramburo [c], M.A. Leach [a], N.P. Brandon [b], T.C. Green [c], C.S. Adjiman [b,d]

[a] *Centre for Energy Policy and Technology, Imperial College London, London SW7 2AZ, UK*
[b] *Department of Chemical Engineering and Chemical Technology, Imperial College London, London SW7 2AZ, UK*
[c] *Department of Electrical and Electronic Engineering, Imperial College London, London SW7 2AZ, UK*
[d] *Centre for Process Systems Engineering, Imperial College London, London SW7 2AZ, UK*

Received 23 November 2004; received in revised form 9 May 2005; accepted 16 May 2005
Available online 19 July 2005

Abstract

Solid oxide fuel cell combined heat and power (CHP) is a promising technology to serve electricity and heat demands. In order to analyse the potential of the technology, a detailed techno-economic energy-cost minimisation model of a micro-CHP system is developed drawing on steady-state and dynamic SOFC stack models and power converter design. This model is applied it to identify minimum costs and optimum stack capacities under various current density change constraints. Firstly, a characterisation of the system electrical efficiency is developed through the combination of stack efficiency profiles and power converter efficiency profiles. Optimisation model constraints are then developed, including a limitation in the change of current density (A cm^{-2}) per minute in the stack. The optimisation model is then presented and further expanded to account for the inability of a stack to respond instantaneously to load changes, resulting in a penalty function being applied to the objective function proportional to the size of load changes being serviced by the stack. Finally, the optimisation model is applied to examine the relative importance, in terms of minimum cost and optimum stack maximum electrical power output capacity, of the limitation on rate of current density change for a UK residential micro-CHP application. It is found that constraints on the rate of change in current density are not an important design parameter from an economic perspective.

Keywords: Solid oxide fuel cell; Power converter; Cost optimisation; Micro-CHP

1. Introduction

Efficient technologies, such as solid oxide fuel cells are an important link in achieving a low-carbon economy as presented by the UK Government in the Energy White Paper [1]. The White Paper suggests a 60% carbon reduction target by 2050. This is a challenging aspiration, only achievable through a variety of measures including some relating to energy efficiency. In addition to low-carbon aspirations, a substantial complementary effort is being directed at moving towards more decentralised electricity generation. A part of the potential decentralised energy markets is the residential sector, which is a large consumer of both electricity and heat, and could benefit from consolidation to meet these demands via combined heat and power (CHP). Bringing all these points together, this paper develops a techno-economic model for meeting energy demand with micro-CHP using SOFC technology, and applies it to a residential situation.

Appropriate techno-economic characterisation of solid oxide fuel cell micro-CHP technology can provide a useful tool to direct research to improve this technology, and give manufacturers a guide for suitable system design. In this paper, steady-state and dynamic SOFC stack models are used along with a detailed power converter model to develop an accurate high-level characterisation of SOFC-based micro-CHP in the 0–5 kW_e range. This information

* Corresponding author. Tel.: +44 207 594 7312; fax: +44 207 594 9334.
E-mail address: a.hawkes@imperial.ac.uk (A.D. Hawkes).

0378-7753/$ – see front matter © 2005 Elsevier B.V. All rights reserved.
doi:10.1016/j.jpowsour.2005.05.076

is then used to inform a cost minimisation model that calculates the minimum equivalent annual cost of meeting given energy demands, and chooses the optimum stack capacity[1] to install for that energy demand.

Firstly, relevant performance characteristics of the fuel cell stack under consideration – an anode-supported intermediate-temperature direct internal reforming SOFC – are presented. The technical and design requirements for a power converter that produces alternating current from the direct current fuel cell are then considered. The optimisation model, which brings these technical depictions together and reflects them into model inputs and constraints, is then presented. The model is applied to analyse the influence of an upper and lower bound on the change in current density on the minimum cost and optimum micro-CHP system capacities in a residential situation corresponding to a large UK household. This particular analysis is justified in that a greater rate of change in current density in a SOFC stack implies a greater induced temperature gradient across the stack, and therefore a greater induced thermal stress. Given that increased stress is likely to adversely impact on stack lifetime, there is a rationale behind limiting the rate of change of current density such that it is below a certain specified value, and consequently prolonging the lifetime of the stack. As no quantitative basis exists to relate a specific limit on change in current density to a particular cell lifetime a sensitivity analysis across a range of values is performed to inform our conclusions.

2. Solid oxide fuel cell performance

Solid oxide fuel cells [2,3] consist of air and fuel channels, a three-layer ceramic region composed of the anode and cathode separated by a dense electrolyte (PEN structure) and an interconnect structure used to combine cells together. SOFCs operate at high temperatures and atmospheric or elevated pressures, and can use H_2, CO or hydrocarbons as fuel and air as oxidant. In a SOFC, the O^{2-} ions formed at the cathode migrate through the ion-conducting electrolyte to the anode/electrolyte interface where they react with the H_2 and CO contained in (and/or produced by) the fuel, producing H_2O and CO_2 while releasing electrons that flow via an external circuit to the cathode/electrolyte interface. SOFCs can be classified according to their geometry, operating temperature, relative thickness of PEN components or method of processing the fuel. This paper focuses on the performance of planar anode-supported intermediate-temperature (IT) direct internal reforming (DIR) SOFCs. The operating temperature range of IT-SOFCs is from 823 to 1073 K, as compared to the 1073–1273 K range of high-temperature SOFCs. The temperature reduction allows IT-SOFCs to use a wider range of materials and have a more cost-effective fabrication method. Anode-supported SOFCs (where the anode is the thickest PEN component and the electrolyte must have high ionic conductivity and small thickness) have been developed to minimise the high ohmic losses attributed to IT operation. DIR is a possible approach to convert a primary fuel into the H_2-rich gas required by SOFCs. In this approach, the CH_4 is fed directly to the cell and reforming takes place on the anode, eliminating the need for a separate fuel reformer. It is known that DIR in high-temperature SOFCs may lead to steep local cooling effects caused by the endothermic DIR reaction, and can generate large, potentially damaging, temperature gradients. However, the lower operating temperature of IT-SOFCs has been shown to be beneficial as it naturally reduces the DIR reaction rate.

For operation, a SOFC stack must be embedded within a SOFC system incorporating a balance of plant (BoP) to supply air and clean fuel at the appropriate operating conditions, convert the direct current (dc) to alternate current (ac), and remove or process the depleted reactants, products and heat [4–6]. A complete SOFC system is generally composed of five main sub-systems: fuel processing, fuel cell stack, power conditioning, heat recovery and/or further power generation using integrated gas and steam turbines and plant control. For a SOFC system, the starting point is the fuel processing: natural gas is first partially or totally externally steam reformed in a pre-reformer before being fed to the SOFC stack, producing hydrogen and carbon monoxide, both of which can be used by the stack as fuel; any natural gas remaining can be reformed internally in the stack, providing useful cooling. The electrochemical power generation takes place when dc electricity is produced within the fuel cells, normally combined in a varying number of cells or stacks that can match a particular power requirement. The power-conditioning unit converts the electric power from direct current into regulated direct current or alternate network current and is described in more detail in Section 3. The heat recovery unit refers to the recovery of residual heat in the exhaust gas that can be used, for example, to heat water for local space heating, thus giving a higher overall system efficiency. The control sub-system guarantees that both the BoP and the SOFC stack respond rapidly and safely to any variations, such as a change in electrical or thermal load.

2.1. SOFC stack model

References [7] and [8] reported on the development of a dynamic one-dimensional planar co-flow anode-supported IT DIR-SOFC model, which is used here to predict the stack performance. To produce a useful voltage, a SOFC consists of several repeating electrochemical cells in a module, connected both in series and/or in parallel and assembled to compose a stack. However, SOFC models are usually developed

[1] "Stack capacity" is defined as the maximum electrical power output capacity of the SOFC stack and dc–ac converter combined. It therefore includes losses in the dc–ac converter, but does not consider parasitic loads of micro-CHP system. Parasitic loads are accounted for in the optimisation model through inclusion in demand curves, and a percentage power loss (e.g. 5%) on stack/converter output.

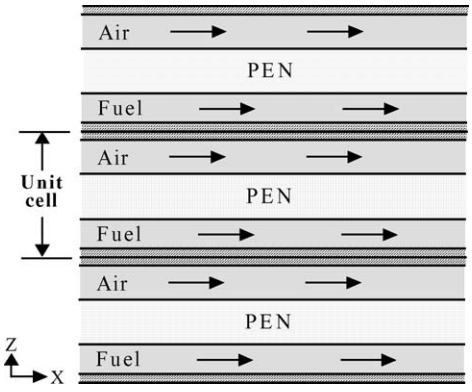

Fig. 1. Schematic side view of a co-flow planar SOFC stack.

for the smallest unit cell or module, then used to compute the operating conditions of the whole stack. In the case reported here, the repeating single-cell is considered to be in the centre of a large stack, such that no edge effects are present, and to be formed when two interconnect plates are placed above and below the cell PEN structure. A schematic side view of a co-flow SOFC stack, where the unit cell being modelled is indicated, is illustrated in Fig. 1. For the model, the SOFC was considered to be composed of fuel and air channels, PEN structure and interconnect. The model consists of mass balances around the fuel and air channels, energy balances around the fuel and air channels, PEN and interconnect and an electrochemical model that relates the fuel and air gas compositions and the various cell temperatures to voltage, current density and other cell variables. The chemical species considered are CH_4, H_2O, CO, H_2 and CO_2 for the fuel stream and O_2 and N_2 for the air stream. It is assumed that only H_2 is electrochemically oxidised, all the CO is converted through the water-gas shift reaction, assumed at equilibrium, and any CH_4 in the fuel can only be reformed to H_2, CO and CO_2 but not electrochemically oxidised. The electrochemical model accounts for ohmic losses across the PEN structure and for anode and cathode concentration and activation overpotentials. The model described is able to predict the various cell temperatures (fuel and air channels, PEN structure and interconnect), the gas composition (fuel and air channels), and all the electrochemical-related variables (open-circuit voltage, activation, ohmic and concentration overpotential losses, terminal potential, output power, current density, etc.) along the cell length as well as their variation with time. Reference [7] presents the developed model and analyses both the electrochemical and steady-state performance of the cell, while reference [8] focuses on the dynamic response of the cell to several current density step-changes and discusses possible control strategies.

2.2. Stack current density, electrical efficiency and dynamic response

To use the information provided by the SOFC model in the present design optimisation analysis, it is necessary to express

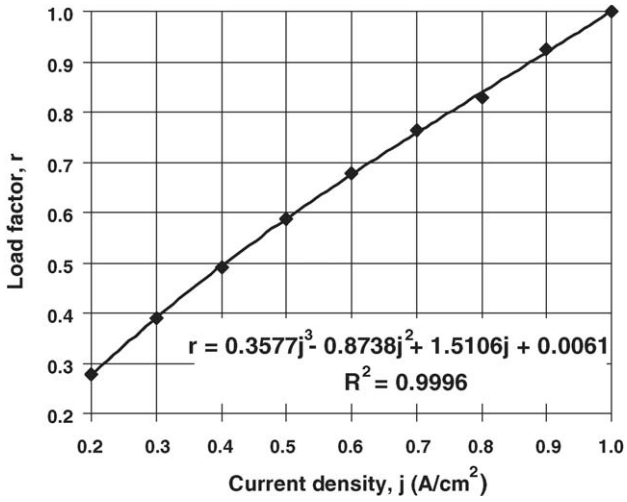

Fig. 2. Load factor vs. current density and corresponding fit function.

the cell efficiency as a function of demand (steady-state current load or current load changes). To do this, a dimensionless parameter, the load factor (r), is used. It is defined as the ratio between the instantaneous power output of the stack and its total capacity (total capacity is defined as the maximum electrical power output of the SOFC stack). For example, if r is 0.5, the stack is operating at 50% of its maximum output capacity. Expressions were developed for the efficiency as a function of the load factor, the load factor as a function of the current density for steady-state conditions and the load factor as a function of both the current density and time when load step-changes occur. For this purpose, the model was used to generate data that was then fitted to appropriate functions that could be integrated into the optimisation problem.

Fig. 2 presents the load factor variation with current density, where a third order polynomial function that fits the data is provided, and Fig. 3 the equivalent information for

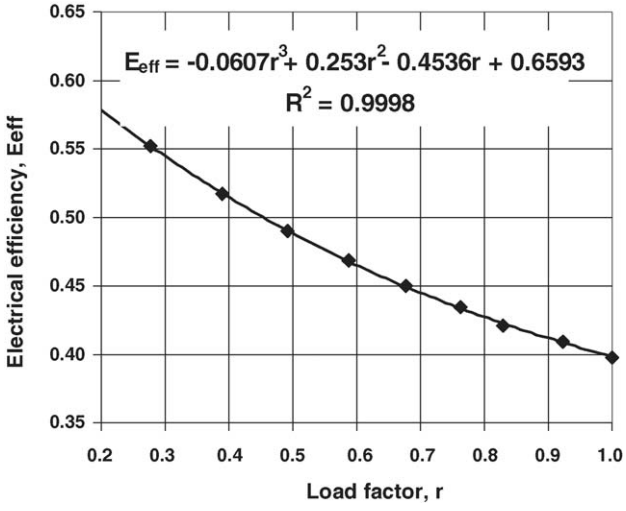

Fig. 3. SOFC stack electrical efficiency (defined as the fraction of the chemical energy in the inlet fuel that is converted to electric power) vs. load factor and corresponding fit function.

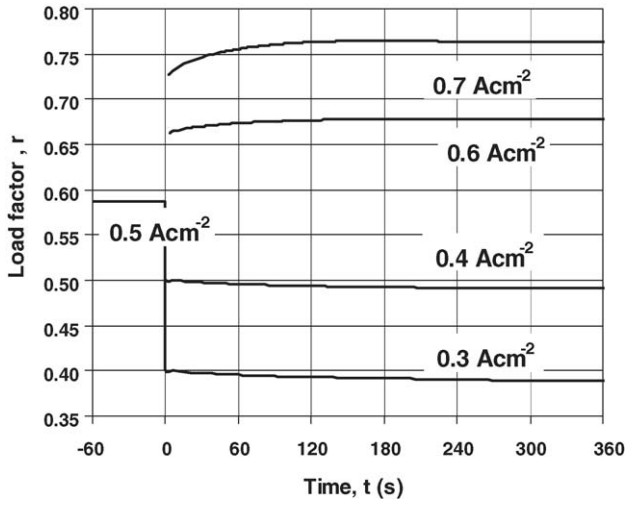

Fig. 4. Transient response of the cell load factor for 0.5 (initial steady-state conditions) to 0.3, 0.4, 0.6 and 0.7 A cm^{-2} load step-changes.

efficiency as a function of load factor. Electrical efficiency is here defined as the fraction of the chemical energy in the inlet fuel that is converted to electric power. The total capacity of the stack has been set to the power output corresponding to a current density value of 1.0 A cm^{-2}, which is equivalent to setting a lower limit of 0.55 V to the cell voltage. The upper limit of the load factor is then equal to 1 (i.e. no overload is allowed), while the lower limit has been set to 0.2 due to the constraint that the stack must at least meet its own parasitic loads. This load factor range implies current densities between 0.14 and 1.0 A cm^{-2}. The data presented assume that the stack performs equally for any total capacity value, i.e. its performance is independent of size. The data are based on a stack model and neglect the effect of the balance of plant on the efficiency and dynamic behaviour of the system.

The data in Figs. 2–4 were obtained by varying the current density values, while maintaining the remaining inlet conditions fixed: operating pressure of 1 bar, inlet fuel and air temperatures of 1023 K, fuel utilisation of 75% and an air ratio of 8.93. The inlet fuel was considered as a gas mixture of CH_4, H_2O, CO, H_2 and CO_2. Its composition was 28.1% CH_4, 56.7% H_2O, 0.5% CO, 12% H_2 and 2.7% CO_2 which resulted from a mixture with a steam to carbon ratio equal to 2 after 10% pre-reforming (meaning that 10% of the initial methane fuel molar content is reformed prior to entering the fuel cell), where the shift reaction is at equilibrium.

Fig. 4 presents the load factor variation with time for the case where various step-changes in load are introduced. The model is such that both the fuel utilisation and the air ratio are kept constant throughout any variation in current density. It can be seen from Fig. 4 that the load factor increases/decreases progressively to the new steady-state value after a positive/negative load change has been imposed. This slow response of the cell load factor results from the fact that the intermediate period between an imposed disturbance and the new steady-state is characterised by an undershoot (for positive load changes) or an overshoot (for negative load changes) of the cell voltage [8]. As is well known, a SOFC is less/more efficient for higher/lower current density values, causing a larger/smaller production of waste heat with a consequent temperature increase/decrease. In addition, it is clear that the changes taking effect have different characteristic response times: changes in gas flow rates and power output are much faster than changes in temperature. These factors explain the undershoot/overshoot phenomena: as immediately after a current density step-change, the cell temperature is still low/high, all the sources of voltage loss are higher/lower at that point. Therefore, during that intermediate period, the cell voltage is lower/higher than the new steady-state value.

3. Power electronics

3.1. System description

A power conditioning unit (PCU) has, in broad terms, three main goals within a residential SOFC system: (1) convert the dc voltage from the stack to ac, (2) regulate the voltage at its own output terminals to make it useful to the user and (3) prevent any operating condition that may result in damage to the SOFC.

The schematic of a feasible PCU is shown in Fig. 5. The inverter (dc/ac converter) on the left hand side of the diagram is a standard full-bridge single-phase inverter which can be driven by a standard modulation technique [9]. The output of the inverter is connected to a low-pass filter which suppresses the high frequency electrical noise introduced by the switching action of the power transistors. The output of the filter is then connected to a step-up transformer. This transformer is necessary because the dc voltage of the stack is low and does not allow the inverter to produce directly ac voltage of the magnitude need for connection to the distribution grid. In the example considered here a transformer step up ratio of approximately 17 is required to reach the standard single phase distribution voltage of 230 V. The coupling inductance ensures a smooth power exchange between the PCU, the load and/or the grid.

In the PCU considered in this paper, a capacitor is placed between the stack output and the inverter so that the high frequency current components required by the inverter flow through the capacitor rather than the SOFC stack. There are, however, additional benefits of placing capacitance at this point, such as the reduction of either the transient impact on the SOFC of a step change in electrical load or the impact of a SOFC-related voltage disturbance on the electrical network.

3.2. PCU control scheme

The operation of power converters for grid-connected and stand-alone applications is a well documented field [9–11] and only the basic concepts are presented here.

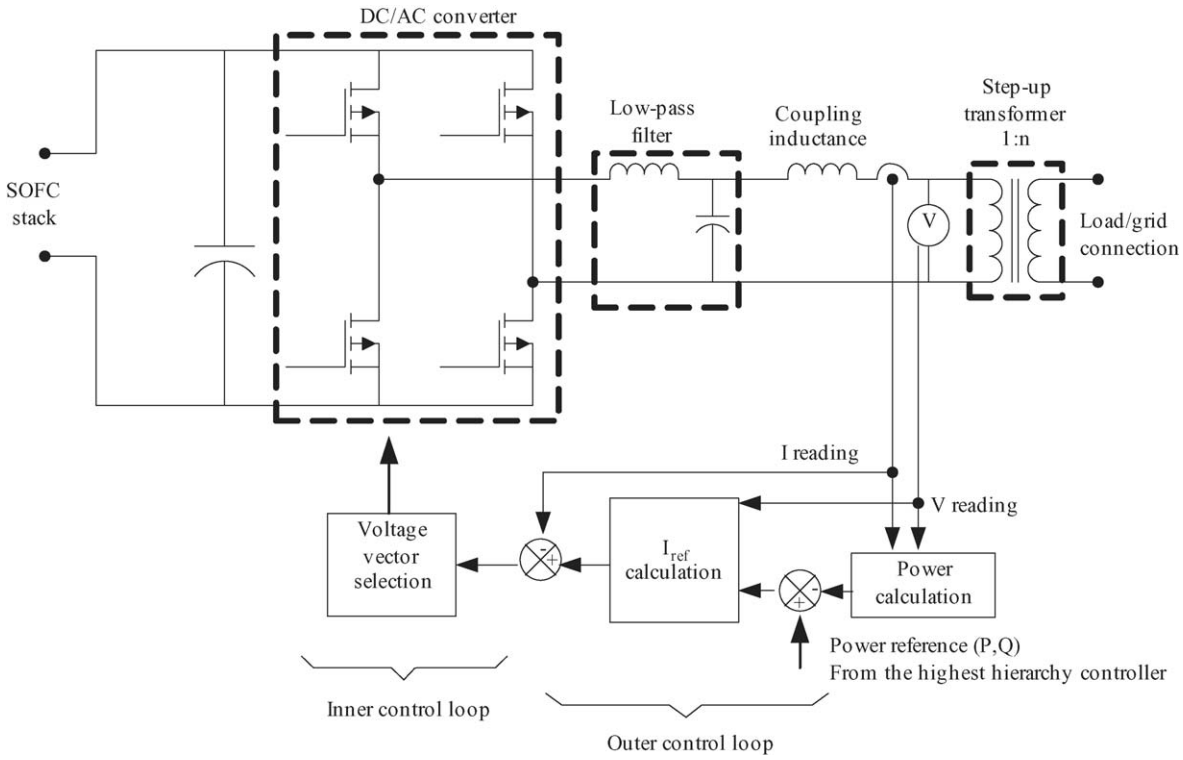

Fig. 5. Schematics of a power conditioning unit.

In a stand alone application the PCU is usually works in voltage control mode. In this mode of operation, the PCU dictates of the quality of the voltage provided to the user. This task normally involves the dynamic compensation of the several voltage-drops that occur across the whole system.

In a grid-connected application, as considered in this paper, the control strategy for the PCU is based on a current control mode. As shown in the lower part of Fig. 5, there are several stages to the control hierarchy. At the highest level, a supervisory control for the whole system sets the real and reactive power to be exported into the electrical network. The actual power export can be calculated and compared with the demand. This assessment allows a calculation to be made of the current export required. This then forms the reference for the inner control loop that forces this current to flow using current feedback and selection of an appropriate voltage vector.

In either operation mode, voltage-controlled or current-controlled mode, the current that flows must be limited so that it does not exceed the physical limits of any of the components of the SOFC-PCU system.

3.3. Efficiency characterisation

The efficiency of the PCU shown in Fig. 5 may be estimated by multiplying the efficiency of the inverter times the efficiency of the step-up transformer. The expected efficiency of a transformer is normally readily available from manufacturers and an example of these performance curves is shown in Fig. 6 [12]. However, the efficiency of a power converter against its loading is not normally found in its technical datasheets. For this reason, the efficiency of the inverter was calculated from as follows.

First, several power ratings were specified (0.5, 1.0, 1.5, 2.0, 3.0, 4.0 and 5.0 kW) and for every power rating a set of appropriate power devices was chosen. For every rated power, several operating conditions were specified (from a low to a high load factor) and from these conditions an output current waveform was estimated (assuming a constant

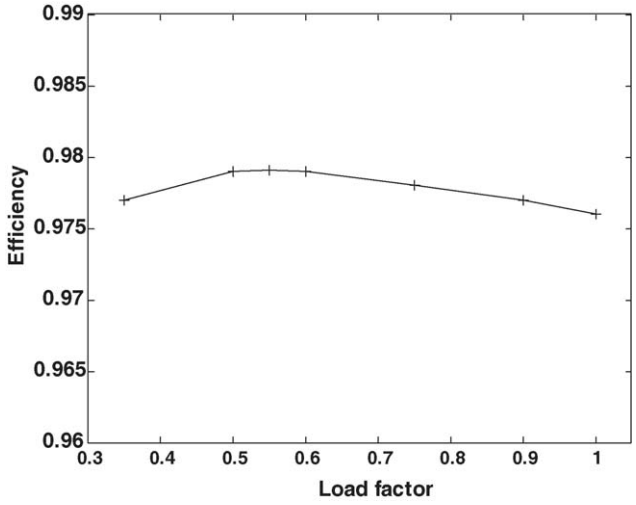

Fig. 6. Efficiency of a transformer against its load factor.

output voltage and no phase displacement between current and voltage). With this current waveform, the value for the dc voltage and a typical switching pattern in the ac/dc converter, the inverter power losses were finally calculated. The calculated losses were the result of summing up the contribution of the three loss phenomena: (1) the switching losses of the power transistors, (2) the reverse recovery losses in the diodes and (3) the conduction losses in both the power transistors and diodes. These loss phenomena are represented by the set of Eq. (1) [13].

$$
\begin{aligned}
P^{\mathrm{D}}_{\mathrm{cond}} &= \frac{1}{T}\int^{t_{\mathrm{off}}} V_{\mathrm{F}} I_{\mathrm{F}}\,\mathrm{d}t \\
P^{\mathrm{Q}}_{\mathrm{cond}} &= \frac{1}{T}\int^{t_{\mathrm{on}}} V_{\mathrm{CEsat}} I_{\mathrm{CE}}\,\mathrm{d}t \\
P^{\mathrm{Q}}_{\mathrm{on}} &= E_{\mathrm{on}} f_{\mathrm{sw}} \qquad P^{\mathrm{Q}}_{\mathrm{off}} = E_{\mathrm{off}} f_{\mathrm{sw}} \\
P_{\mathrm{rr}} &= E_{\mathrm{rr}} f_{\mathrm{sw}} = Q_{\mathrm{rr}} V_{\mathrm{dc}} f_{\mathrm{sw}}
\end{aligned}
\tag{1}
$$

$P^{\mathrm{D}}_{\mathrm{cond}}$ and $P^{\mathrm{Q}}_{\mathrm{cond}}$ are the conduction power losses in the diodes (D) and transistors (Q), respectively, $P^{\mathrm{Q}}_{\mathrm{on}}$ and $P^{\mathrm{Q}}_{\mathrm{off}}$ the switching power losses in the transistors, E_{on}, E_{off} and E_{rr} the energy loss per commutation operation during the turn-on process, turn-off process and reverse recovery effect, correspondingly, V_{F} and I_{F} the forward voltage and current of the diodes, V_{CEsat} the saturation voltage of the transistors and I_{CE} the conduction current, V_{dc} the dc-link voltage and Q_{rr} is the reverse recovery charge. The data fed into Eq. (1) are taken from the datasheets of several devices [14].

A further fixed power loss was added to the other power converter operating losses to account for the power requirement of the microprocessor-based control system and for cooling (ventilation) losses. This power loss overhead was estimated from experience with other power converters of similar ratings, ranging from 8 W (for the small converters) to 15 W (for the larger ones).

Several efficiency curves for the PCU are plotted in Fig. 7 against the output power. Each curve corresponds to a particular power rating (and a respective set of power devices), from curve 1 to 7: 0.5, 1.0, 1.5, 2.0, 3.0, 4.0 and 5.0 kW. These efficiency curves already include the efficiency of the transformer (extrapolated to a load factor of 0.2).

The information presented in Fig. 7, is difficult to handle in an optimisation routine because it is discrete in nature. Fig. 8 shows the same values of efficiency of Fig. 7 but plotted against the load factor. This figure suggests that an approximation for the efficiency performance of a "generic" converter may be obtained by taking the average of the several curves. This average is shown in Fig. 8 with a bold dashed line.

There are a number of PCU topologies available to choose from in addition to that shown in Fig. 5. The particular architecture chosen for a PCU depends on the optimisation targets the designer sets: low capital (or development) cost, power loss minimisation, volume (and weight) minimisation and reliability maximisation are examples among many targets.

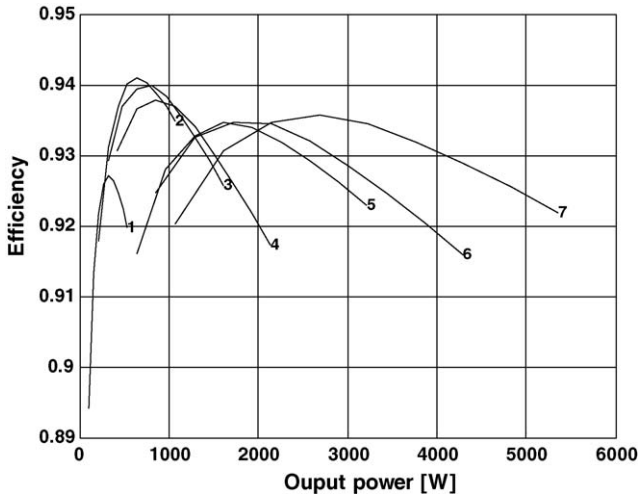

Fig. 7. Efficiency for several power converters plotted against their output power (Curve 1 = 0.5 kW, 2 = 1.0 kW, 3 = 1.5 kW, 4 = 2.0 kW, 5 = 3.0 kW, 6 = 4.0 kW, 7 = 5.0 kW).

A topology may include, for example, the use of a high-frequency transformer (operated at several kHz) in place of a 50/60 Hz transformer. The physical size of a transformer per unit of power is inversely proportional to its operating frequency and operating the transformer at higher frequency can significantly reduce its volume and cost. However, a critical comparison of the efficiencies obtainable by the available topologies is still an issue open for discussion. The topology for the PCU presented in this paper is a representative example chosen to illustrate the characteristics of the efficiency associated with a power converter.

3.4. Electrical energy storage

As pointed out previously, there are several time constants involved in the production of electricity by a SOFC and, as a

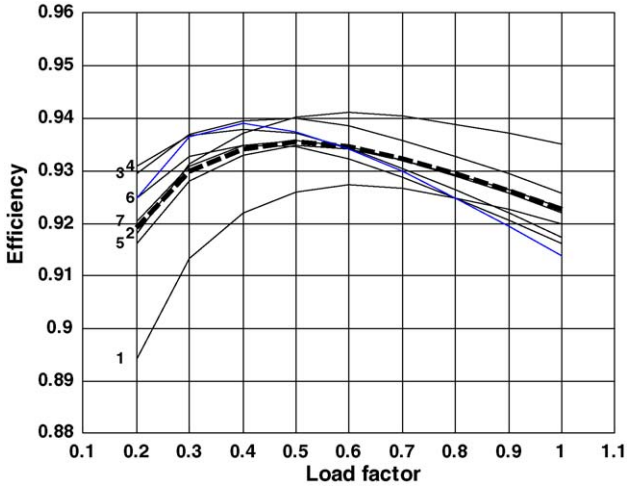

Fig. 8. Efficiency for several power converters plotted against the load factor (Curve 1 = 0.5 kW, 2 = 1.0 kW, 3 = 1.5 kW, 4 = 2.0 kW, 5 = 3.0 kW, 6 = 4.0 kW, 7 = 5.0 kW).

consequence, the system may take some time to respond to sudden changes in electrical load. These abrupt changes may be compensated, or smoothed, by storing energy in another device. The selection of the storage technology depends heavily on the application in mind, and it may become a complex process of balancing out costs, benefits, physical size and required performance for a given time scale [15].

From a general point of view, electrical energy storage may play different roles in a SOFC system. It can be designed to compensate for the transients in the system (milliseconds to minutes range), to provide a fault ride-through capability to the user (minutes range) or perhaps to peak shave the consumer demand curve (hours range).

To illustrate the compromises involved in the selection of a storage device, consider that compensation of the chemical response during a load step is required. Upon consideration of Fig. 4, it is clear that this response time is in the milliseconds range. In this time scale, capacitors connected between the SOFC and the inverter would be a reasonable choice. However, the size and lifetime of the capacitors may be of concern. For this topology, the capacitors may have to handle high currents and this has serious implications for the size, cost and reliability of the PCU. Capacitors with suitable current rating can be large and the stressful operating conditions imposed by high currents are normally handled well only by good quality (and usually expensive) capacitors. For the thermal transient (minutes range), capacitors are clearly not an appropriate choice.

Batteries could be considered in place of capacitors since they have a higher energy density and could provide additional power for a longer period. However, most battery technologies do not possess the right combination of power capability and energy capacity for this application. In addition, a battery management system could be required, increasing the capital cost of the system. Other forms of energy storage (such as fly-wheels or super-capacitors) exhibit similar or equally restrictive disadvantages.

All this suggests that several forms of storage might technically be able to compensate for the millisecond-range transients, but it is unlikely to be cost competitive with simply exchanging compensating power with the grid. It was therefore decided to proceed with the grid-only energy compensation strategy (and the dynamic response penalty function is developed later in the paper for this purpose).

4. Micro-CHP cost minimisation model

4.1. Model definition

The cost minimisation model employed is designed to optimise a grid-connected micro-CHP system consisting of a SOFC stack, power electronics module and a supplementary boiler to meet rapid changes in heat demand (such as some domestic hot water demands) that may not be met by the stack. The model minimises the equivalent annual cost (EAC) of meeting given electricity demand and heat demand profiles that represent an entire year of energy consumption through the choice of six appropriate sample days [16]. The equivalent annual cost consists of equivalent annual capital costs, annual maintenance costs, annual fuel costs for the stack and the supplementary boiler, annual electricity import costs and is partially offset by annual revenue from electricity export.

Optimisation decision variables are stack maximum electrical output capacity, y (kW_e), supplementary boiler capacity, v (kW_{th}), stack electrical output, x_i (kWh), natural gas consumption by the supplementary boiler, z_i (kWh), electricity import, w_i (kWh) and electricity export, u_i (kWh), for each time period under analysis ($i = 1, 2, 3, \ldots, n$). Therefore, the optimisation routine chooses the best design capacities for the components of the micro-CHP system, and shows how this plant would be optimally dispatched under the given energy demand profiles.

4.2. Smoothed load factor definition

In order to allow optimal choice of the stack maximum electrical generation capacity, it is necessary to define many quantities with respect to the stack load factor. The smoothed load factor, r_i, is defined as the ratio of average stack electricity output in time period i to the stack's maximum electricity output, and is simply a smoothed version of the load factor mentioned in previous sections. The smoothed load factor defined here is numerically stable as the stack output in any time period, x_i, and the stack capacity, y, tend toward zero. The smoothed load factor r_i is defined as per Eq. (2), where r_{lim} is a limiting value of r (to control behaviour of the function at stack capacities where machine precision is significant) and ε is a typical round-off error of y^2.

$$r_i(x_i, y) = \sqrt{\frac{x_i^2 + r_{\text{lim}}^2 \varepsilon}{y^2 + \varepsilon}},$$
$$\text{for each time period } i = 1, 2, 3, \ldots, n. \tag{2}$$

This function provides a numerically smooth load factor under conditions of varying load and varying stack capacity. The value of r_{lim} is set to 0.5, whilst ε depends on the precision of the computer in use, but is usually of the order 1×10^{-16}. Consequently, as x_i and y tend to zero, the load factor smoothly tends towards operation at half-capacity, but where y is greater than zero operation at any load factor between 0 and 1 is numerically stable and r_{lim} and ε terms' influence are negligible.

4.3. System efficiency

The determination of the micro-CHP system electrical efficiency requires the combination of the SOFC stack electrical efficiency curve, and the power converter efficiency curve. These two curves have been defined in Figs. 3 and 8, respectively. An empirical system electrical efficiency is generated

by multiplying the stack efficiency by the power converter efficiency for each value of r. A polynomial fit is then applied to generate a smooth approximation of the system efficiency curve as shown in Fig. 9.

The curve in Fig. 9 displays the high part-load efficiency of a fuel cell system, and the effect of the power converter is more apparent at low load factors. The polynomial fit is very accurate apart from at these low load factors, but these are relatively unimportant for the present problem as our stack is limited to operate above a load factor (r) of 0.2.

4.4. Optimisation objective function

4.4.1. Construction of the objective function

The objective function minimised represents the equivalent annual cost of meeting a given energy demand, defined by a set of sample days that are used to represent electricity and heat demand for an entire year. Each sample day consists of a number of time periods which have associated electricity and heat demand (kWh). All sample days are considered simultaneously, represented by a total of n time periods.

Cost drivers for meeting the energy demand are the cost of fuel for the stack and the supplementary boiler, the cost of electricity imported from the grid, plant maintenance costs per kWh produced, plant maintenance costs per year, revenue from electricity sale to the grid and capital costs of the stack and the supplementary boiler. Eqs. (3) and (4) represent these cost drivers (C), where g_i is the cost per kWh of natural gas, e_i is the cost per kWh of electricity, p_i is the price given per kWh of electricity export to the grid, $\mathrm{om_B}$ and $\mathrm{om_S}$ are the supplementary boiler and stack maintenance costs per kWh, $\mathrm{aom_B}$ and $\mathrm{aom_S}$ are the supplementary boiler and stack fixed maintenance costs per year, and $\mathrm{af_S}$ and $\mathrm{af_B}$ are the annuity factor over the lifetime of each piece of equipment under a given discount rate. η_{Se} and η_{B} are the electrical efficiency of the stack and efficiency of the boiler, respectively.

$$C_{\mathrm{Fixed}} = \frac{\tanh(Ay)(H(y) + \mathrm{aom_S})}{\mathrm{af_S}} + \frac{\tanh(Bv)(I(v) + \mathrm{aom_B})}{\mathrm{af_B}} \tag{3}$$

$$C_{\mathrm{Variable}} = \sum_{i=1}^{n} \left(w_i e_i + z_i g_i + \frac{x_i g_i}{\eta_{\mathrm{Se}}(r_i)} + x_i\,\mathrm{om_S} + z_i \eta_{\mathrm{B}}\,\mathrm{om_B} - u_i p_i + D_i \right) \tag{4}$$

The coefficients A and B in Eq. (3) dictate how quickly capital and annual maintenance costs tend to zero as each capacity tends to zero, resulting in a smooth (twice continuously differentiable) capital cost and annual maintenance cost function. The functions H and I represent the capital cost of the stack and boiler, respectively, in terms of capacity. The coefficient D_i in Eq. (4) is a dynamic response penalty function designed to penalise a stack that meets rapid electrical load changes, and is defined in Section 4.4.2. The total

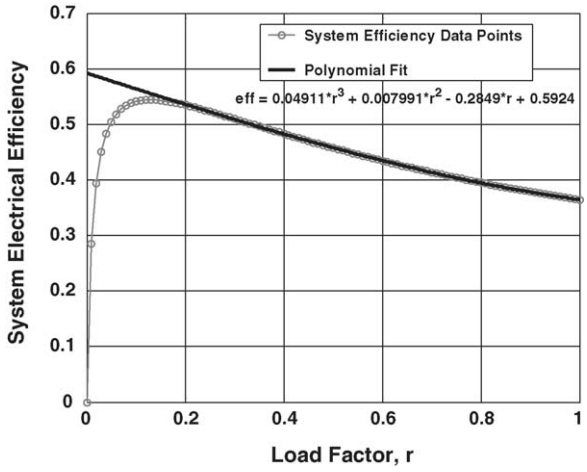

Fig. 9. Micro-CHP system electrical efficiency vs. load factor.

equivalent annual cost of the system is given by the sum of capital and variable costs as per Eq. (5).

$$\mathrm{EAC} = C_{\mathrm{Fixed}} + C_{\mathrm{Variable}} \tag{5}$$

4.4.2. Dynamic response penalty function

Upon consideration of Fig. 4, it is apparent that the SOFC stack can not respond to 100% of an electrical load change instantaneously, and as noted, dynamic response is characterised by voltage undershoot and overshoot for positive and negative load changes, respectively. Chemical response times are of the order of 300 ms, followed by the thermal transient until a steady state is reached after a few minutes. The chemical response is effectively instantaneous with respect to the time-frame modelled (one power output decision variable per minute), but the thermal transients warrant the introduction of additional terms in the objective function to correct for the slightly altered costs of meeting energy demand when there is energy interchange with the grid/boiler implied by a load step-change (where the stack can not respond quickly enough within a time period). To model this phenomenon, as a simplification, it is assumed that only a certain percentage, P, of the load change, Δx_i (defined as x_{i+1}–x_i for all $i = 1, 2, 3, \ldots, n-1$), can be met by the stack, and therefore there exists a small overhead of $1-P$ percent of Δx_i that must be traded with the grid and a corresponding influence on the source of heat delivery. The energy traded with the grid can be either import or export, depending on the onsite demand at the time of the step-change, and the magnitude of the onsite load. The electricity exchanged with the grid is characterised by four cases:

1. Positive load step-change, final stack output greater than onsite load. There is an implied loss of revenue as the complete load step-change is not met immediately and therefore some electricity is not exported.
2. Positive load step-change, final stack output less than onsite load. Implies that a slow response will require additional energy to be imported from the grid.

3. Negative load step-change, final stack output less than onsite load. There is an implied avoided cost as less electricity is imported from the grid.
4. Negative load step-change, final stack output greater than onsite load. A slow response means additional electricity is exported to the grid.

Similar to these four cases, heat demand met by the stack/boiler needs to be corrected as per the following two cases. Note that cases pertaining to stack heat output greater than the onsite heat demand impose no economic penalty.

1. Positive load step-change, final stack heat output less than onsite heat demand. There is an implied penalty as the supplementary boiler must meet the heat load not met due to slow response of the stack.
2. Negative load step-change, final stack heat output less than onsite heat demand. There is an implied gain as the stack meets some additional heat load.

The penalty imposed by these six cases is approximated by the three discontinuous functions defined by Eqs. (6)–(8), where the average stack overall efficiency (heat plus power) is given by $\eta_{\text{So, average}}$, the average stack electrical efficiency is $\eta_{\text{Se, average}}$, HD_i is the heat demand in time period i and ED_i is the electricity demand in time period i.

$$D_i = p_i(1-P)\Delta x_i - g_i(1-P)\frac{\Delta x_i}{\eta_{\text{Se, average}}},$$
$$\text{for } \text{ED}_{i+1} < x_{i+1}, \tag{6}$$

$$D_i = e_i(1-P)\Delta x_i - g_i(1-P)\frac{\Delta x_i}{\eta_{\text{Se, average}}},$$
$$\text{for } x_{i+1} < ED_{i+1}, \tag{7}$$

$$D_i = \left(\frac{\eta_{\text{So, average}}}{\eta_{\text{Se, average}}} - 1\right)\frac{g_i}{\eta_{\text{B}}}(1-P)\Delta x_i,$$
$$\text{for} \frac{\eta_{\text{So, average}}}{\eta_{\text{Se, average}}} x_{i+1} - x_{i+1} < \text{HD}_{i+1} \tag{8}$$

Combining Eqs. (6)–(8), and applying smoothing terms (S_e and S_h) to deal with discontinuities yields Eq. (9), where a dictates the gradient of the penalty function close to the discontinuities.

$$D_i = (1-P)\Delta x_i \left[e_i(-S_e + 0.5) + p_i(S_e + 0.5) - \frac{g_i}{\eta_{\text{Se, average}}} + \left(\frac{\eta_{\text{So, average}}}{\eta_{\text{Se, average}}} - 1\right)\frac{g_i}{\eta_{\text{B}}}(S_h + 0.5)\right] \tag{9}$$

where $S_e = 0.5\tanh(a(x_{i+1} - \text{ED}_{i+1}))$ and $S_h = -0.5\tanh\left(a\left(\left(\frac{\eta_{\text{So, average}}}{\eta_{\text{Se, average}}}x_{i+1} - x_{i+1}\right) - \text{HD}_{i+1}\right)\right)$

4.4.3. Further discontinuities in the objective function

In addition to the discontinuities associated with capital cost, annual maintenance cost, and the penalty function overcome through use of a hyperbolic tangent function, the objective function defined in Eq. (5) may contain some discontinuities due to the nature of common energy pricing structures. A residential energy tariff is often constructed through charging a certain price per kWh initially in a quarter, and then lowering the price per kWh once the cut-off consumption level has been achieved. Therefore, the gradients of energy prices are discontinuous, causing difficulties in minimising the objective function using a sequential quadratic programming (SQP) method which requires a smooth function (twice continuously differentiable). However, a SQP method will often only run into difficulties where the price discontinuity is near the problem solution. As this occurrence is rare, no smoothing function is provided to alleviate the discontinuity, and advent of a solution near a discontinuity is flagged in the model implementation.

4.5. Optimisation constraints

4.5.1. Heat constraint

The first non-linear constraint in this optimisation problem formulation is that heat demand must be satisfied or exceeded by a certain value corresponding to the system's potential to dump excess heat, usually through a fan-assisted flue. Eq. (10) defines the non-linear part of this constraint (the linear part is defined by the supplementary boiler efficiency), where HD_i is the heat demand in time period i, θ is the allowable heat dump and r_i is the smoothed load factor over time period i.

$$\text{HD}_i < G_i(x_i, r_i(x_i, y)) < \text{HD}_i + \theta,$$
$$\text{for each time period } i = 1, 2, 3, \ldots, n \tag{10}$$

The stack's heat output in this problem is dictated by the stack overall efficiency (heat plus power) $\eta_{\text{So}}(r_i)$, the stack electrical efficiency $\eta_{\text{Se}}(r_i)$ and the stack electrical output x_i. Therefore, G is defined as per Eq. (11).

$$G_i(x_i, r_i(x_i, y)) = \frac{\eta_{\text{So}}(r_i)}{\eta_{\text{Se}}(r_i)}x_i - x_i,$$
$$\text{for each time period } i = 1, 2, 3, \ldots, n \tag{11}$$

For the micro-CHP system under consideration, the relationship between electrical efficiency and load factor is defined in Fig. 9. The overall efficiency, $\eta_{\text{So}}(r_i)$, is particular to the pinch point design of the technology, and for the present case is defined later in the input data section.

4.5.2. Change in current density constraint

In order to place a constraint on current density for an optimisation problem that includes stack capacity as a decision variable it is necessary to define current density as a function of the smoothed load factor r_i. The constraint function is defined as per Eq. (12), where C_1 and C_2 are the maximum allowable negative and positive change in current density j

between time periods, respectively.

$$C_1 < F_i(r_i, r_{i+1}) = j_{i+1} - j_i < C_2,$$

$$\text{for each time period } i = 1, 2, 3, \ldots, n-1. \quad (12)$$

The function F in Eq. (12) is defined by considering the relationship between load factor and current density described by Fig. 2. Substituting and transforming (to give j in terms of r) this relationship results in Eq. (13).

$$F_i(r_i, r_{i+1}) = -0.1162r_{i+1}^3 + 0.5388r_{i+1}^2 + 0.5815r_{i+1} + 0.1162r_i^3 - 0.5388r_i^2 - 0.5815r_i \quad (13)$$

As the sequential optimisation routine performance is significantly improved by the provision of constraint gradients, these are derived using the chain rule as per Eqs. (14) and (15).

$$\frac{\partial F}{\partial x_i} = \frac{\partial F}{\partial r_i}\frac{\partial r_i}{\partial x_i} \quad (14)$$

$$\frac{\partial F}{\partial y} = \frac{\partial F}{\partial r_i}\frac{\partial r_i}{\partial y} + \frac{\partial F}{\partial r_{i+1}}\frac{\partial r_{i+1}}{\partial y} \quad (15)$$

The constraint limits C_1 and C_2 in Eq. (12) may now be set to desired levels, resulting in corresponding constraints on r_{i+1} according to r_i for each time period under analysis.

4.5.3. Linear constraints

The linear constraints in this model formulation are straight-forward. Firstly, electricity balance must be respected as per Eq. (16), where ED_i is the electricity demand in time period i, and other variables are as defined above. Secondly, system capacities must not be exceeded for the stack or the supplementary boiler as per Eqs. (17) and (18), with variables as defined above.[2]

$$ED_i = x_i + w_i - u_i,$$

$$\text{for each time period } i = 1, 2, 3, \ldots, n \quad (16)$$

$$0 \le x_i \le y, \quad \text{for each time period } i = 1, 2, 3, \ldots, n \quad (17)$$

$$0 \le z_i\eta_B \le v, \quad \text{for each time period } i = 1, 2, 3, \ldots, n \quad (18)$$

5. Results and discussion

5.1. Input data

Results obtained here have been obtained through running the model with the following input economic data and technical data as defined above:

1. SOFC stack capital cost: £333 kW_e^{-1} + £333 basic cost.
2. Supplementary boiler capital cost: £50 kW_{th}^{-1} + £1000 basic cost (minimum 5 kW_{th}).
3. SOFC stack lifetime: 5 years.
4. Supplementary boiler lifetime: 10 years.
5. SOFC stack annual maintenance cost: £20.
6. Supplementary boiler annual maintenance cost: £45.
7. Energy tariffs:
   (a) Gas: 2.309 p(kWh)$^{-1}$ for first 1143 kWh quarter^{-1}, 1.453 p(kWh)$^{-1}$ thereafter.
   (b) Electricity: 10.49 p(kWh)$^{-1}$ for first 225 kWh quarter^{-1}, 6.38 p(kWh)$^{-1}$ thereafter.
8. Electricity export price: 3 p(kWh)$^{-1}$.
9. Discount rate: 12%.
10. Maximum heat dump: 0.5 kW.
11. Six selected days of energy demand data, with data points for each minute ($n = 8640$).
12. Overall system efficiency (heat plus power) $\eta_{So}(r_i) = 0.05r + 0.9$
13. Dynamic response $P = 95\%$.

The other input of interest is the load profile. Electricity and heat demand profiles that correspond to a large UK household have been chosen for this analysis. The electricity demand data was supplied by the Building Research Establishment Ltd. (BRE) from a residential photovoltaic field trial, and the heat demand data was developed from aggregate consumption information combined with an assumed heating cycle in winter months of the year, and an assumed domestic hot water load.

According to the UK Department of Trade and Industry, average residential electricity consumption was approximately 4700 kWh per year per dwelling in the UK in 2003 [17,18]. Average gas consumption was 19,961 kWh in Great Britain in 2002 [19], of which approximately 10% is accounted for by cooking. The household which is considered in this analysis exhibits larger than average consumption, having 7627 kWh electricity demand and 24,539 kWh heat demand (excluding cooking). The average daily electricity load factor (in this case, the maximum demand in a day divided by average demand for that day) is 0.11, with the 99th percentile of annual demand occurring at approximately 7 kW. The average daily thermal load factor is 0.14, and maximum demand in the year is 25.6 kW.

5.2. Results

The sensitivity of the minimum equivalent annual cost to the rate of change of current density is investigated by imposing a limit on this change of 0.002, 0.01, 0.05, 0.1, 0.2, 0.3 and 0.4 A cm^{-2} min^{-1}, and finally essentially no constraint on the rate of change of current density (implemented by a 1.0 A cm^{-2} min^{-1} constraint). In order to analyse the influence of this constraint on a pre-existing system, the stack capacity is initially fixed at 1 kW_e, and the supplementary

[2] Note that v and y are adjusted to represent their maximum output over the time period in question. For example, if a time period lasts for 1 min, a 1 kW_e stack would be able to deliver a maximum of 0.016667 kWh of energy.

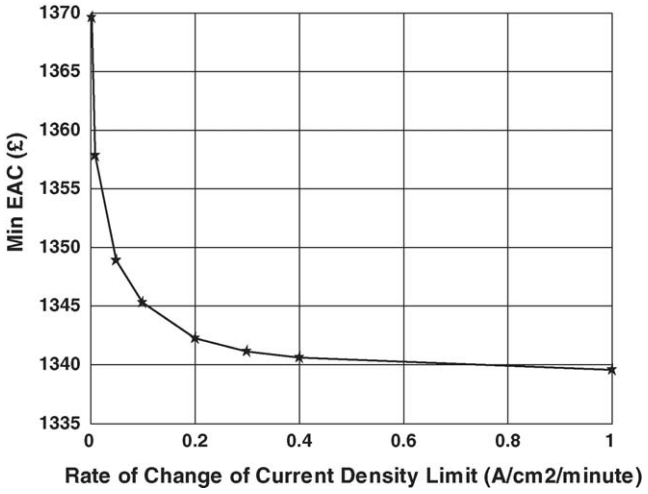

Fig. 10. Minimum equivalent annual cost vs. limit on the rate of change of current density.

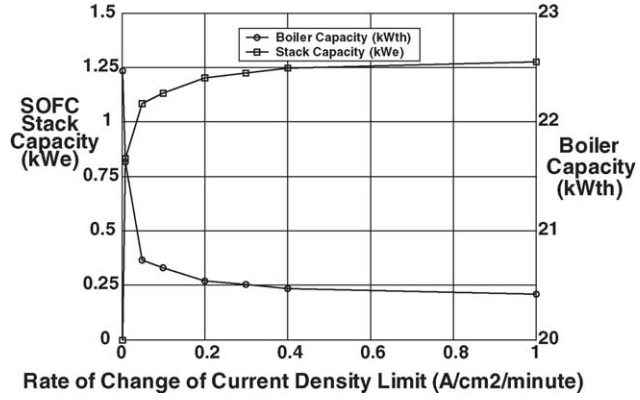

Fig. 11. Optimum system capacities vs. limits on the rate of change of current density.

boiler capacity is fixed at a value that can service the entire heat demand. Fig. 10 shows the minimum equivalent annual cost obtained for a large UK dwelling, across the range of current density change limits investigated.

Another set of calculations is carried out in which the optimum stack and boiler capacities are determined for each current density constraint to examine their influence on the design and manufacturing strategy (based on the attractiveness of the system to an investor). Fig. 11 shows optimum system capacities for the same large UK dwelling demand profile as investigated in Fig. 10.

To provide a basic understanding of the system energy flows, the optimum systems in Fig. 11 would have resulted in the figures estimated in Table 1.

5.3. Discussion

The result displayed in Fig. 10 indicates the relatively small impact on minimum EAC of relaxing the constraint on current density. For this dwelling, the difference between a 0.002 A cm^{-2} min^{-1} limit and no constraint is £30 per year. This value corresponds to approximately 2% of the equivalent annual cost of meeting energy demand. This suggests that the micro-CHP stack's response to load changes is not an important design parameter from an economic perspective. Therefore, if constraining current density increases the lifespan of a stack, the designer should note that additional lifetime is almost certainly more valuable than the ability to service a rapid change in current density.

Fig. 11 provides insight into the influence of the constraint on current density on optimum system capacities. The trend is intuitive; as current density changes become more constrained, optimum stack capacity decreases whilst optimum supplementary boiler capacity increases. The constraint on change in current density limits the ability of the stack to meet larger heat and electricity loads, as the time taken for ramp-up often exceeds the duration of the loads. Therefore, the economic effectiveness of the stack becomes more limited at high loads because the marginal cost of increasing stack capacity approaches and eventually exceeds the marginal benefit obtained from operating that extra capacity.

For the dwelling considered in Fig. 11, the "no constraint" optimum stack capacity of 1.25 kW_e is almost reached when the change in current density limit is 0.3 A cm^{-2} min^{-1}, and only descends below 1 kW_e when the change in current density limit is 0.01 A cm^{-2} min^{-1}. This investor would choose a boiler-only system when change in current density is limited to 0.002 A cm^{-2} min^{-1}—the minimum value in this analysis.

Other studies have shown that this result is highly dependent on the combination of input parameters utilised [20], and any change in these could yield a different result regarding investment attractiveness. However, it is expected that approximately the same result for the change in EAC (approximately 2% of the EAC between maximum and minimum limits) with respect to the various rate of change of current

Table 1
Optimum system energy flows for two example cases of rate of change of current density constraint

Rate of change of current density limit (A cm^{-2} min^{-1})	Annual electrical energy generated by stack (kWh (% onsite demand))	Annual heat energy generated by the stack (kWh (% onsite demand))	Annual electrical energy imported to the site from the grid (kWh)	Annual electrical energy exported from the site to the grid (kWh)
0.01	4600 (60%)	4500 (18%)	3480	355
Unconstrained	6100 (80%)	6700 (27%)	2650	1020

density limits would be achieved over a wide range of input parameters (i.e. the shape of Fig. 10 will remain approximately the same). Also note that the results presented are based on the integration of different components (fuel cell stack, boiler and power conditioning unit), but no attempt has been made to optimise the overall system.

6. Conclusion

An interdisciplinary cost-minimisation model for meeting a given energy demand using solid oxide fuel cell stack based micro-CHP has been presented, drawing on steady-state and dynamic stack modelling, and power converter design. Technical aspects of the stack performance and power converter design have been considered to formulate an electrical efficiency profile for the system. As temperature gradients in a solid oxide fuel cell stack produce stress in integrated materials, and since the rate of change in current density is linked to temperature gradients, a current density constraint has been developed for the cost-minimisation model. This current density constraint effectively imposes limits on the change in power output level for the stack, reducing its ability to respond in the way which would produce least cost if the stack were unconstrained.

The model was then applied to analyse residential grid-connected micro-CHP for the case of electricity and heat demand for a large UK household. It was found that constraining the current density has little impact on the minimum cost of meeting this residential energy demand, with a difference of only £30 per year, between the most constrained case and the unconstrained case for a fixed 1 kW_e stack system. This result is useful when considering dispatch strategy and design of SOFC micro-CHP, as it is apparent that an investor would be nearly indifferent between equally long-lived stacks that have significantly different constraints on the rate of change in current density. When the possibility that a tightly-constrained stack is longer-lived than an unconstrained stack is considered, an investor becomes more likely to pursue the tightly-constrained case.

When considering optimum system capacities, it has been shown that the constraint on rate of change in current density has limited impact on results. The change in optimum stack capacity between the "no constraint" case and the 0.05 $A\,cm^{-2}\,min^{-1}$ cases is less than 0.25 kW_e. The supplementary boiler capacity exhibits similar behaviour, increasing only slightly as the rate of change in current density constraint is tightened. These results further reinforce the point that tight constraints on current density are relatively unimportant in terms of investment attractiveness, and a manufacturer/designer could choose an appropriate stack capacity and associated rate of current density change constraint, and be reasonably assured that the investment attractiveness of the technology would not be changed significantly if they had chosen an alternative (nearby) limit on rate of change in current density.

Acknowledgements

The Engineering and Physical Sciences Research Council who have provided funding for this work is gratefully acknowledged. Additionally, thanks to BRE Ltd. for the provision of electricity demand data, and Dr. Evatt Hawkes for assistance in developing smoothing function for the optimisation modelling.

References

[1] British Crown, Energy White Paper: Our Energy Future—Creating a Low Carbon Economy, Report No. Cm5761, Department of Trade and Industry, London, UK, 2003 (see also: http://www.dti.gov.uk/energy/whitepaper/ourenergyfuture.pdf).
[2] K. Kordesch, G. Simader, Fuel Cells and Their Applications, New York, VCH, 1996.
[3] N.Q. Minh, T. Takahashi, Science and Technology of Ceramic Fuel Cells, Elsevier, Amsterdam, 1995.
[4] K. Jonn, Fuel cells—a 21st century power system, J. Power Sources 71 (1998) 12–18.
[5] EG&G Technical Services, Parsons Inc., Science Applications International Corporation. Fuel Cell Handbook, fifth ed., U.S. Department of Energy, Office of Fossil Energy, National Energy Technology Laboratory, Virginia, 2000.
[6] J. Padullés, G.W. Ault, J.R. McDonald, An integrated SOFC plant dynamic model for power systems simulation, J. Power Sources 86 (2000) 495–500.
[7] P. Aguiar, C.S. Adjiman, N.P. Brandon, Anode-supported intermediate-temperature direct internal reforming solid oxide fuel cell. I. Model-based steady-state performance, J. Power Sources 138 (2004) 120–136.
[8] P. Aguiar, C.S. Adjiman, N.P. Brandon, Anode-supported intermediate-temperature direct internal reforming solid oxide fuel cell. II. Model-based dynamic performance and control, J. Power Sources 147 (2005) 136–147.
[9] N. Mohan, T.M. Undeland, W.P. Robbins, Power Electronics—Converters, Applications and Design, second ed., Wiley & Sons Inc., 1995.
[10] M. Prodanovic, T.C. Green, Control and filter design of three-phase inverters for high power quality grid connection, IEEE Trans. Power Electron. 18 (January (1)) (2003) 373–380.
[11] M. Prodanovic, T.C. Green, Control of power quality in inverter-based distributed generation, in: IEEE 28th Annual Conference of the Industrial Electronics Society IECON'02, vol. 2, 2002, pp. 1185–1189.
[12] Ballard transformers datasheets, see also: http://www.ballard.com (Customdesignedtransformerforpv.pdf) accessed on 22nd September 2004.
[13] B.W. Williams, Power Electronics—Devices, Drivers, Applications and Passive Components, second ed., Macmillan Press Ltd., 1992.
[14] International Rectifier datasheets, see also: http://www.irf.com, Components IRFU3504, IRL 1404S, IRF 2204 and IRF 2804.
[15] L.H. Willis, W.G. Scott, Distributed Power Generation: Planning and Evaluation, Marcel Dekker Inc., 2000.
[16] A. Hawkes, M. Leach, Impacts of temporal precision in optimisation modelling of micro-CHP, Energy 30 (10) (2005) 1759–1779.
[17] National Statistics, Energy in Brief July 2003, Department of Trade and Industry, London, UK, 2003, p. 15 (see also: http://www.dti.gov.uk/energy/inform/energy_in_brief/index.shtml).

[18] National Statistics, Census 2001, National Statistics (undated) London, UK (see also: www.statistics.gov.uk).
[19] National Statistics. Energy Trends December 2003, Department of Trade and Industry, 2003, p. 28 (see also: http://www.dti.gov.uk/energy/inform/energy_trends/index.shtml).
[20] A. Hawkes, M. Leach, SOFC systems for the micro-CHP market—modelling key characteristics and sensitivities, in: Proceedings of Fuel Cell Seminar, 1–4 November, San Antonio, USA, 2004.